23rd ABCM International Congress of Mechanical Engineering
December 6-11, 2015, Rio de Janeiro, RJ, Brazil

NUMERICAL STUDY OF A FLUID DYNAMIC ON A BLADE OF WINDMILL WITH EMPHASIS ON THE TORQUE

Morgana de Vasconcellos Araújo
Edjan Tomaz da Silva
Antonio Gilson Barbosa de Lima
Federal University of Campina Grande. Rua Aprigio Veloso, 882. Bairro Universitario. Campina Grande-PB. Code Zip: 58.429-900.
e-mails: morganamva@gmail.com, edjants@gmail.com, gilson@dem.ufcg.edu.br.

Luciano Leite de Sousa
Mauricio de Nassau College. Rua Antonio Carvalho de Souza, 295. Estação Velha Campina Grande-PB. Code Zip: 58.410-050
e-mail: luciano.engenhariabrasil@gmail.com.

Leonardo Pereira de Lucena Silva
Sebastião Araújo Coutinho
Suna Engenharia. Rua Sabino de Farias, 138. Bairro do Quarenta. Campina Grande – PB.
e-mails: leonardo@sunaengenharia.com.br, sacoutinho@sunaengenharia.com.br

Abstract. *With the current renewable energy demand and due to current energy crisis, the wind energy takes place on the world energy scenario. The wind energy has been exploited for centuries in various forms, from ancient windmills to modern wind turbines. The windmill is a wind machine that was first used in grinding grain and irrigation, and to this day is still used for water pumping, and, therefore, have been used in rural areas nowadays. The aim of this paper is study the fluid dynamic of the wind on the blade of a windmill. Was simulated the flux of air on a blade in a three dimensional domain. Were established a stationary domain and a rotative domain. The numerical simulation is done using the commercial package ANSYS CFX 12.1. The turbulence model used was the model Shear Stress Transport. The torque changing with the velocity of the wind and with the attack angle is analyzed, as well as the field of forces and pressures on the blade.*

Keywords: *Numerical Simulation, Windmill, Blade, Torque.*

1. INTRODUCTION

The wind has been used like a form of energy for a million years. Historic records of more than 5 thousand years show the use, by ancient Egyptians, of the wind to surf on Nilo River. The first record wrote about wind energy was done by Heron of Alexandria approximately in the year of 62, using windmill to activate a musical instrument organ. The first Persian windmills were registered in 6 b.C. and they are present again in that region.

The multiblade windmill were developed in the United States of America between 1850-1860 by Daniel Halladay, one of the first manufacturer. The windmill was the first wind turbine manufactured in the world and with the aims of water pumping.

The first windmill projected for generate electricity in a large scale was idealized by Charles F. Brush in 1888 and implement in Cleveland, Ohio. The system is composed by a rotor with 17 m in diameter and built with wood blades. The gear box transmitted movement in a ratio 50:1, reaching 500 rpm. The hardiness, big solidity and low velocities produced only 12 kW.

In the year of 1973 the first turbine of modern era was installed in the North American state of Ohio, having a rotor with two blades with 38 m in diameter and producing 100 kW of power. Nowadays, there are some wind farms to produce energy in wide scale, where the turbines reach 100 m of rotor diameter. But, the production of energy in a small scale is a challenge yet.

Recent studies on the windmill technology are hard to find, since the windmill is an old equipment and its use is in most facing to the pumping of water. In the case of wind machines, in recent decades the science comes valuing the development and improvement of wind turbines, which are electric power generation equipment.

Fagbenro *et al.* (2013) simulated in two dimensions the wind flow on windmill blades, studying lift and drag coefficients of the profile, velocity and kinetic energy fields, plus the cascate effect, which studies the influence of the presence of other blades in the rotor on the air mass flow. Tezuka *et al.* (2008) studied the pressure distribution around a two-dimensional windmill blade profile.

For the development of the present work, a research about methodologies of wind turbine analysis in computational fluid dynamic was done. A standard for three-dimensional analysis is observed. Lanzafame *et al.* (2013) studied a wind turbine in a cylindrical domain. The rotor has two blades and a diameter of 10.058 m. On the domain were built a polyhedral mesh with 9 million elements. They used the turbulence model Shear Stress Transport. Were adopted a speed rotation of 72 rpm and the authors compared lift and drag coefficient with experimental data.

Abdelsalam *et al.* (2014) studied a wind turbine in a parallelepiped domain. The rotor has three blades and a diameter of 82 m. On the domain were built a tetrahedral mesh with 5.7 million elements. They used the turbulence model κ–ε. Were adopted a speed rotation of 17.1 rpm and the authors compared speed profile and noise with experimental data.

Abrar *et al.* (2014) studied a micro wind turbine in a parallelepiped domain. The rotor has three blades and a diameter of 23.65 cm. On the domain were built an adaptive mesh with 10.4 million elements. They used the turbulence model κ–ε. Were adopted speed wind from 4 m/s and for each simulation there is a wind speed with a speed rotation. The main objective is find a pitch angle that gives a bigger torque.

Choi *et al.* (2014) studied the effect of the wake caused by a wind turbine on the other turbine. Two horizontal axis turbines were arranged in a parallelepiped domain, by the way to simulate a wind farm. The rotors have three blades and a diameter of 84.2 m. On the domain were built a tetrahedral mesh with 9.6 million elements. They used the turbulence model Shear Stress Transport. Were adopted a speed rotation of 18.7 rpm, a tip speed ratio of 7.5 and an inlet velocity of wind of 11m/s. The main objective is analyzing the fields of velocity, pressure and turbulence.

Luz (2012) studied a wind turbine in a parallelepiped domain. The rotor has two blades profile NREL S809 and a diameter of 10 m. On the domain were built a tetrahedral mesh with 2.25 million elements. Were adopted a speed rotation of 72 rpm and were used value of 5, 7 and 9 m/s for the wind speed. The main objective is analyzing the turbulence models κ–ω and Shear Stress Transport.

This work aims to study one blade of windmill, analyzing the pressure and the force field on the blade surface, beyond the torque on the blade. The attack angle of wind and the wind velocity were changed. The mean purpose is to find the attack angle that will produce the biggest torque for, in the future, change the position of blade to reach a better production of energy.

The windmill taken as a reference was constructed by Yvel factory, has 18 blades with a 60 ° angle of attack and its rotor has a radius of 1.5 m. The Yvel factory is located in the city of Campina Grande, in the state of Paraíba, Brazil.

For the cited analyzes, were done numerical simulations of a wind flux on the blade using the commercial package ANSYS CFX 12.1®. The turbulence model Shear Stress Transport were used. All the simulations were done in a laboratory called Laboratório Computacional de Térmicas e Fluidos (LCTF) located at Federal University of Campina Grande.

2. MODEL OVERVIEW

The aerodynamic profile of a blade in a turbine have a big contribuition in generating energy. The wind touch the blade, making a boundary layer on this surface. This layer is directly responsible about the distribuition of drag and lift forces on the blade, and this forces command the rotation of rotor. The vector of relative velocity of wind makes a angle with the chord line of the blade, and this angle is called attack angle. For each model of blade there is a maximum angle in wich there are drag and lift. If the angle reach bigger values, there is the deatachment of boundary layer on the surface and the lift dramatically reduces and, consequently, the efficiency of turbine is reduced too, because the lift force is the responsible to give angular velocity to the blade.

The power that can be extracted from the wind is calculated from the Equation 1 (given by Burton *et al.* (2001)):

$$P_W = \frac{1}{2}\rho A V_\infty^3 \tag{1}$$

Where ρ is the air density, A is the area total of the rotor and V_∞ is the wind velocity.

3. METHODOLOGY

3.1 Study Domain

The first domain is a blade with the dimensions showed in the Figure 1. The blade were done using the software Autodesk Inventor 2015 and then exported to ANSYS ICEM CFD. The blade is inserted in a cylindrical domain that has a section of inlet and a section outlet (Figure 2).

For the study of attack angle, the blade was positioned differently, like showed in Figure 3. For it, the spin of the blade around the axis y was needed. The representative mesh of the domain was generated using the block strategy, which a single block is initially created involving the area of study and then the block is subdivided into several others. This strategy allows greater control of mesh refinement in regions desirable. The mesh was refined on the geometry and contains approximately 685000 control volumes as shown in Figure 4, in which illustrates the mesh on a domain with a blade positioned in an attack angle of 30°. For each position of blade was built one mesh.

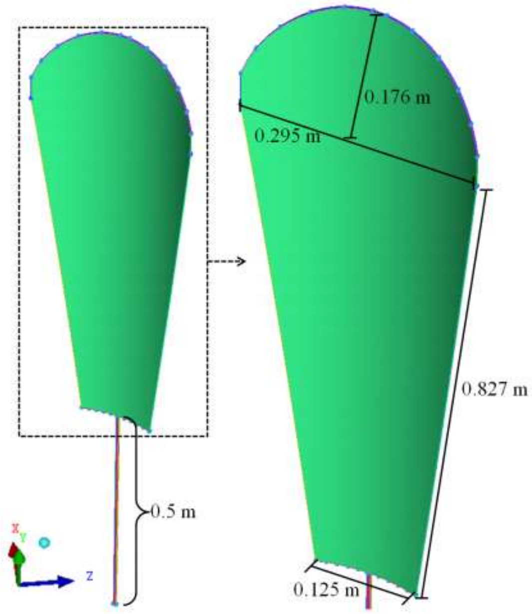

Figure 1. Geometry of blade

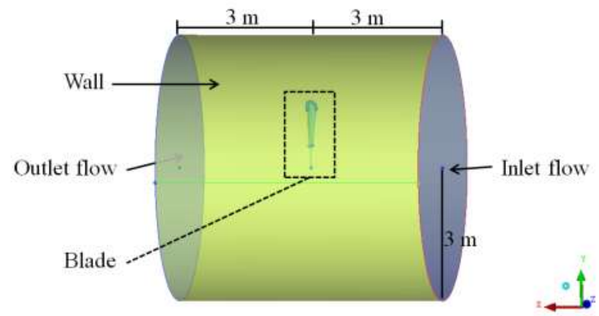

Figure 2. Cylindrical domain with the blade

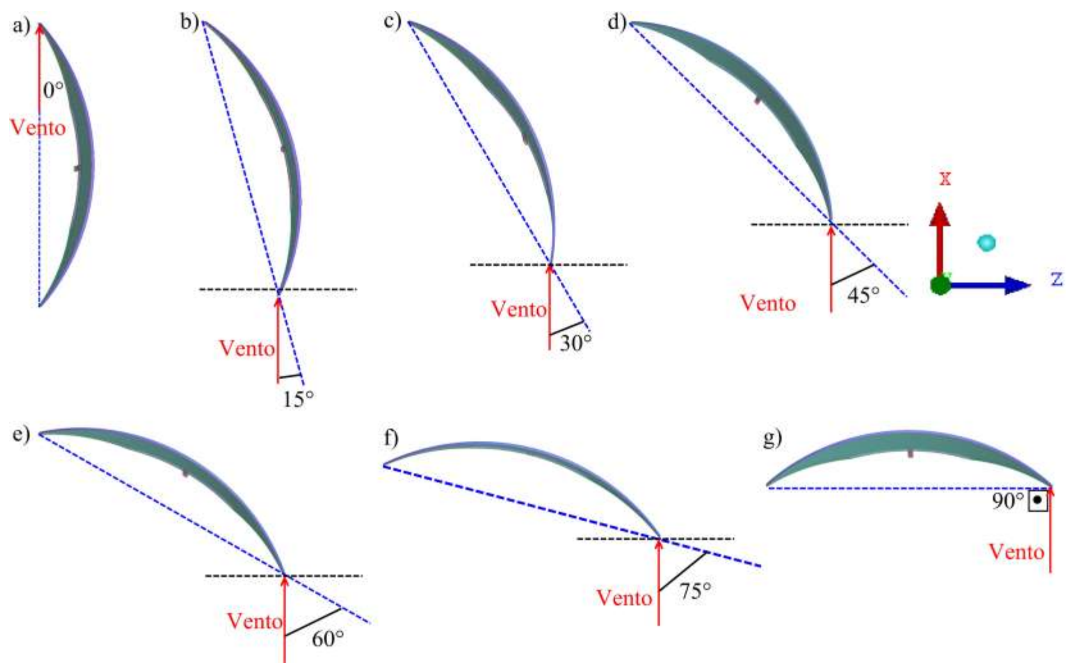

Figure 3. Blade in attack angle of (a) 0°, (b) 10°, (c) 20°, (d) 30°, (e) 45°, (f) 50°, (g) 55°, (h) 60°, (i) 75° e (j) 90°.

3.2 Mathematical Modeling

The studied flow is based on the following considerations:

- Newtonian and incompressible fluid;
- Steady state and isothermal flow;
- Turbulent flow;
- The walls of the equipment are static and smooth;
- There is no occurrence of chemical reactions;

- It was not considered the gravitational effect;

The transport equations that describe the flow were withdrawn in the manual of CFX 12.1. With these considerations, mass and momentum conservation equations are reduced to:

- Mass conservation equation

$$\nabla \cdot \left(\rho U\right) = 0 \quad (2)$$

Where ρ and U are, respectively, the density and the velocity vector.

- Momentum conservation equation

$$\nabla \cdot \left(\rho U \otimes U\right) + \nabla p + \nabla \cdot \tau = 0 \quad (3)$$

Where p is the pressure and τ is the stress tensor.

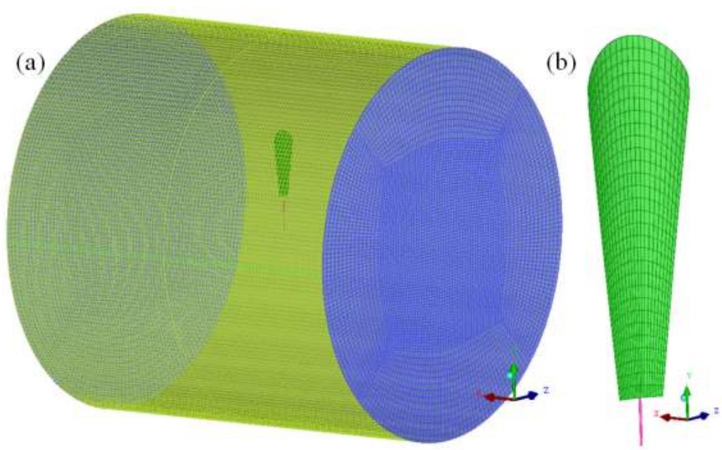

Figure 4. Mesh built on (a) the domain and (b) details of refinement on the blade.

- Turbulence model

With the presence of a turbulent flow inside the device, the mass and momentum equations (Equations 1 and 2) aren't able to adequately predict the oscillations arising from this phenomenon. In addition to the equations of conservation, it is necessary to use a suitable turbulence model. The behavior of the boundary layer on the surface of an airfoil influences directly the intensity of lift and drag forces, and is directly responsible for the movement of the airfoil. The creation of the model *SST* allows an appropriate transport of the shear stress, thus resulting in improved predictions of separation gradient under various conditions, justifying its use. Noleto (2006) shows the transport equations of κ–ω *SST* model like:

$$\frac{\partial\left(\rho\kappa\right)}{\partial t} + \frac{\partial}{\partial x_j}\left(\rho U_j \kappa\right) = \frac{\partial}{\partial x_j}\left[\left(\mu + \frac{\mu_t}{\sigma_\kappa}\right)\frac{\partial k}{\partial x_j}\right] + P_{\kappa b} - \beta`\kappa\omega\rho \quad (4)$$

$$\frac{\partial\left(\rho\omega\right)}{\partial t} + \frac{\partial}{\partial x_j}\left(\rho U_j \omega\right) = \frac{\partial}{\partial x_j}\left[\left(\mu + \frac{\mu_t}{\sigma_\omega}\right)\frac{\partial \omega}{\partial x_j}\right] + \alpha\rho S^2 + \beta\rho\omega + 2\left(1 - F_1\right)\rho\sigma_{\omega 2} + \frac{1}{\omega}\frac{\partial k}{\partial x_j} \quad (5)$$

Where κ is the turbulent dissipation and ω is the turbulent frequency.

For the model were adopted a limiter to the value of the turbulent kinematic viscosity:

$$\nu_t = \frac{a_1 \kappa}{\max\left(\alpha_1\omega, SF_2\right)} \quad (6)$$

Where S is an invariant measure of strain rate, F_1 and F_2 are mixtures of functions based on the distance to the wall and on the flow variables.

3.3 Boundary conditions

The physic-chemical properties of air used in this study are shown in Table 1.

The simulations were performed to analyze the behavior of the torque caused by wind on the blade changing with the attack angle. For it, were organized the cases shown in Table 2. The wind speed is in the range from 3 to 5 m/s. The rotation speed is 0.

Table 1. Fluid data used in all simulation

Parameters	Air
Density [kg/m³] [1]	1.185
Viscosity [Pa.s] [1]	1.831×10^{-5}
Molar mass [kg/kmol] [1]	28.96

[1] Manual of CFX

Table 2. Fluid data used in all simulation

Case	Attack Angle	Wind Speed	Case	Attack Angle	Wind Speed	Case	Attack Angle	Wind Speed
A3	0°	3 m/s	C4	30°	4 m/s	E5	60°	5 m/s
A4	0°	4 m/s	C5	30°	5 m/s	F3	75°	3 m/s
A5	0°	5 m/s	D3	45°	3 m/s	F4	75°	4 m/s
B3	15°	3 m/s	D4	45°	4 m/s	F5	75°	5 m/s
B4	15°	4 m/s	D5	45°	5 m/s	G3	90°	3 m/s
B5	15°	5 m/s	E3	60°	3 m/s	G4	90°	4 m/s
C3	30°	3 m/s	E4	60°	4 m/s	G5	90°	5 m/s

4. RESULTS AND DISCUSSION

4.1 Velocity Magnitude

For the analysis of the of the wind speed around the blade, where plotted velocity fields on the plane at y = 1 m (Figure 5). These fields are shown in the Figure 6. The fields with a wind speed of 3 m/s in the inlet domain are enough to the analysis, because the behavior of the fields with wind speed of 4 and 5 m/s have qualitatively similar behavior.

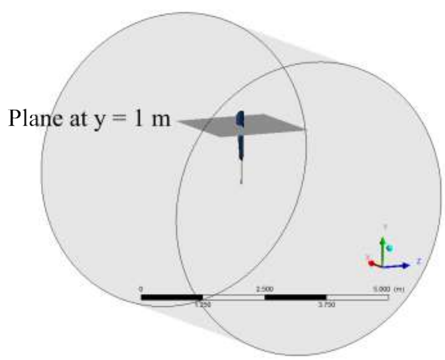

Figure 5. Plane at y = 1 m used for the analysis of velocity, speed and streamlines fields

Note that the region behind of blade shows the lowest velocities, characterizing the wake region. As seen in Figure 6, the simulation results indicates that the flow across blades with different attack angles results in significant differences in the mean velocity distribution of the turbine wakes. See that the cases with the biggest attack angle shown the largest wakes.

The wind speed around the blade can be studied with streamlines, like shown in the Figures 7, 8 and 9. The first discrete signals turbulence begin to occur at an attack angle of 45 °, but the turbulence is clearly saw in the cases with an angle of 60°, 75° and 90°.

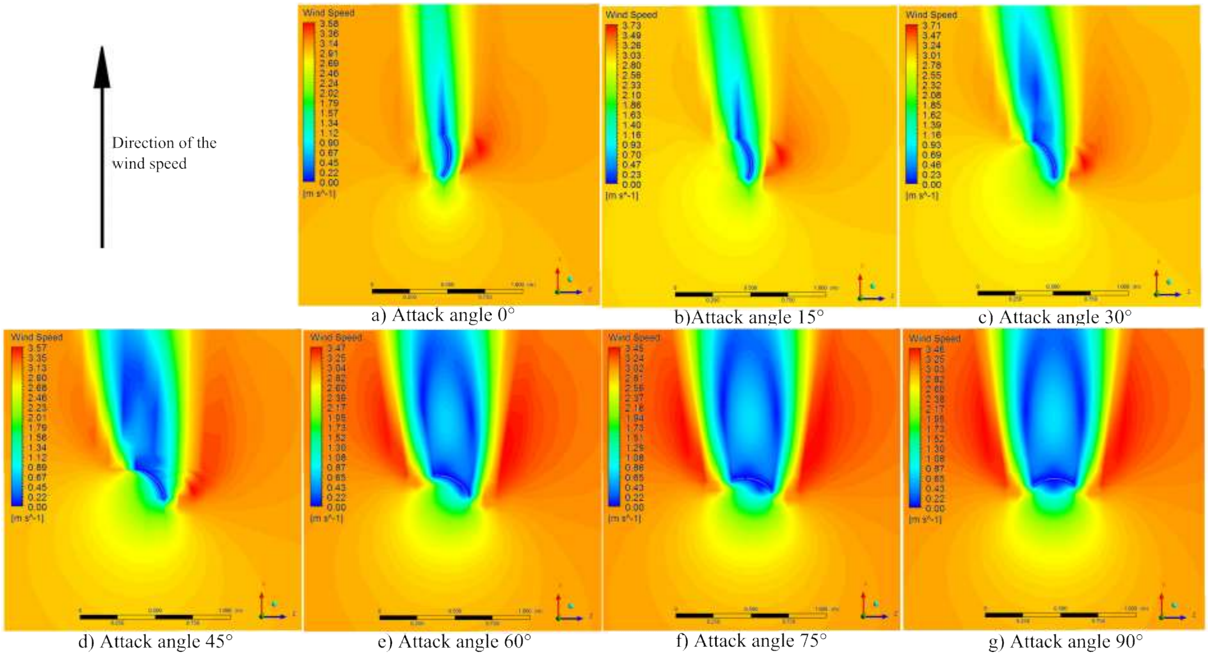

Figure 6. Velocity fields for an inlet wind speed of 3 m/s

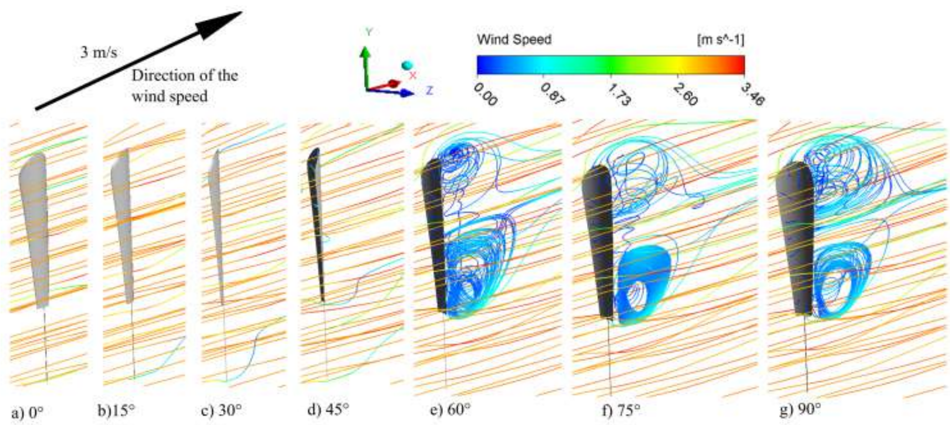

Figure 6. Velocity streamlines around the blade for an inlet wind speed of 3 m/s

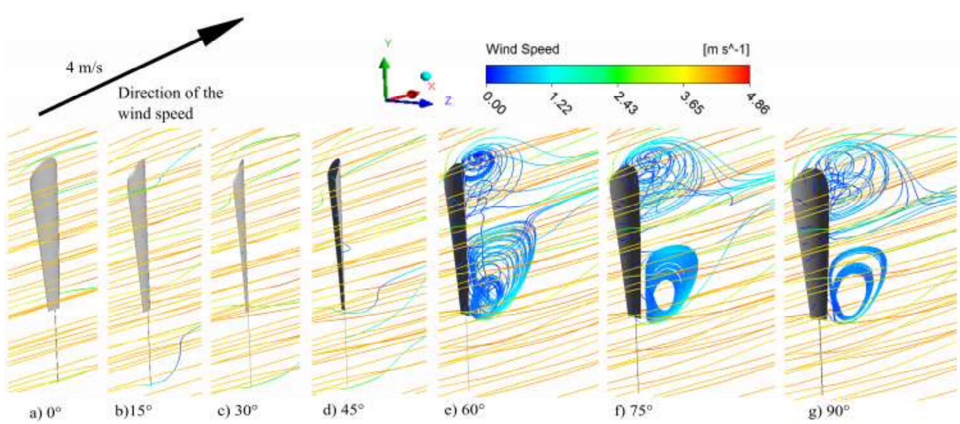

Figure 7. Velocity streamlines around the blade for an inlet wind speed of 4 m/s

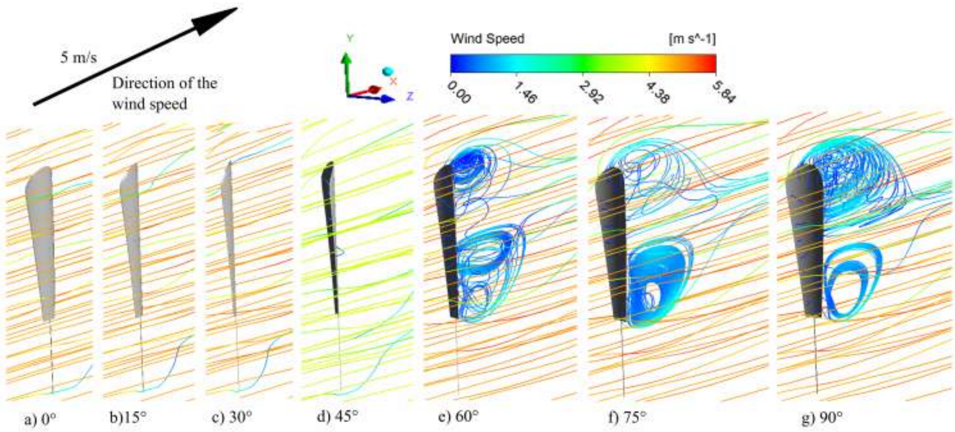

Figure 8. Velocity streamlines around the blade for an inlet wind speed of 5 m/s

4.2 Pressure Field

Analyzing the pressure field shown by the Figure 9 for an inlet velocity of 3 m/s, it is notable that the concave region of the blade undergoes a higher pressure compared to the convex area.

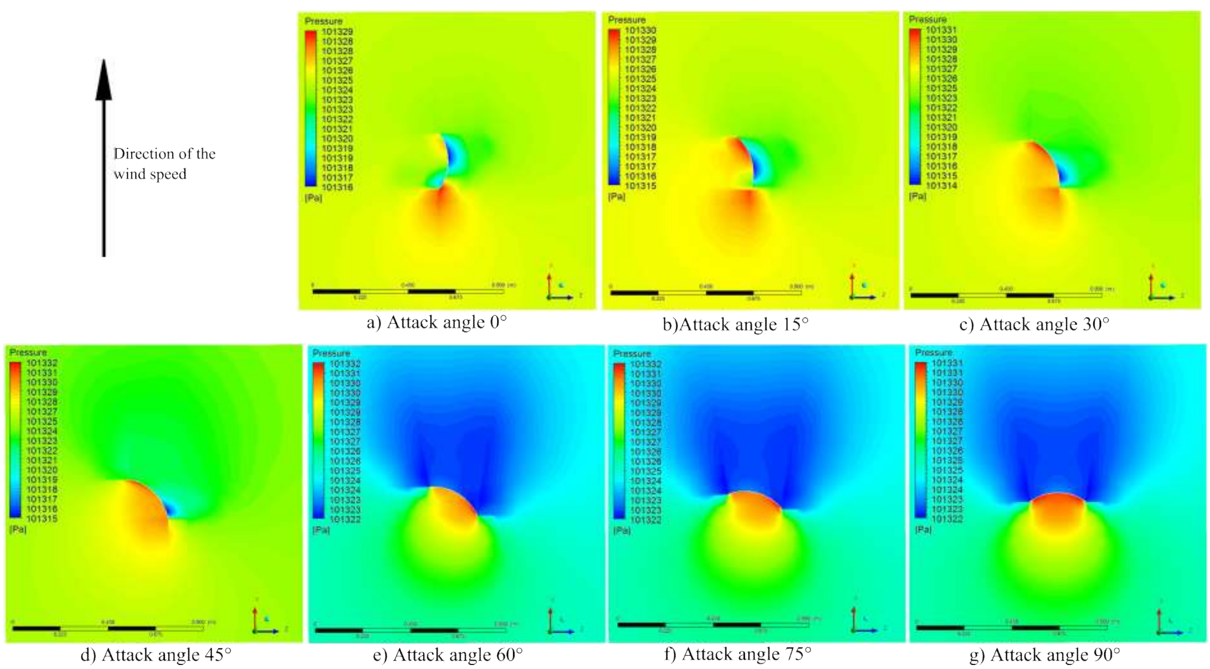

Figure 9. Pressure field around the blade for an inlet wind speed of 3 m/s

4.3 Torque

The wind, when it hits the blade, causes a force on its surface. This force is directly responsible for the torque that drives the rotor rotate. Therefore, the greater is the torque of a blade, the greater is the power extracted from the wind, i.e., the greater is the power produced by the wind generator.

The traditional windmill, as described in the introduction, has blades with attack angle of 60°. The Figure 10 shows the simulation results of the investigation about the torque on the blade in function of the attack angle. Note that for all wind speed simulated, the angle 30° produced the biggest values of torque. For a determined rotational speed, the rotor that will produced a better power will be that one that having blades with angles of attack of 30°.

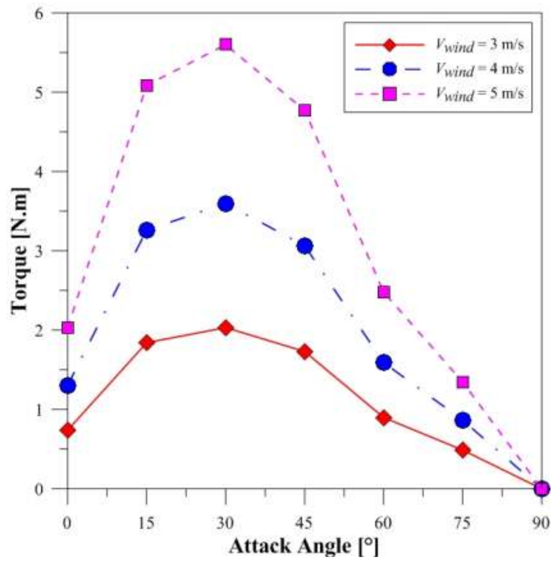

Figure 10. Torque *versus* attack angle

5. CONCLUSIONS

In accordance with the presented results, we conclude that:

- The profile of the velocity field changes significantly with the position of the blade in domain;
- An increase in attack angle causes a turbulence zone behind the blade;
- The higher pressure gradients were observed for larger angles of attack;
- The angle of attack that provided the greatest torque values was 30°.

6. ACKNOWLEDGEMENTS

I would like to thank the LCTF (Laboratório Computacional de Térmicas e Fluidos), belonging to Federal University of Campina Grande, for allowing the use of their computers

7. REFERENCES

Abdelsalam. A. M.; Boopathi, K.; Gomathinayagam, S.; Kumar, S. S. H. K.; Ramalingam, V. 2014. “Experimental and numerical studies on the wake behavior of a horizontal axis wind turbine”. *Journal of Wind Engineering and Industrial Aerodynamics*, Vol. 128, p. 54-65.

Abrar, M. A.; Mahbub, A. M. I.; Mamun, M. 2014. “Design optimization of a horizontal axis micro wind turbine trough development of CFD model and experimentation”. Procedia Engineering, Vol. 90, p. 333-338.

Burton, T.; Sharpe, D.; Jenkins, N.; Bossanyi, E. 2001. *Wind Energy Handbook.* John Wiley & Sons, Chichester.

Choi, N. J.; Nam, S. H.; Jeong, J. H.; Kim, K. C. 2013. Numerical study on the horizontal axis turbines arrangement in a wind farm: Effect of separation distance on the turbine aerodynamic power output. *Journal of Wind Engineering and Industrial Aerodynamics*, Vol. 117, p. 11–17.

Fagbenro, K.A.; Mohamed, M.A. E Wood, D.H., 2014. “Computational modeling of the aerodynamics of windmill blades at high solidity”. *Energy for Sustainable Development*, Vol. 23, p. 1-8.

Lanzafame, R.; Mauro, S.; Messina, M. 2013. “Wind turbine CFD modeling using a correlation-based transitional model”. *Renewable Energy*, Vol. 52, p. 31-39.

Luz, J. L. R. 2012. *Análise Numérica do Desempenho da Turbina Eólica de Eixo Horizontal NREL UAE PHASE VI*. Master dissertation, Federal University of Rio Grande do Sul, Porto Alegre.

Noleto, L. 2006. *Estudo de escoamentos de cilindros: simulação numérica híbrida e grandes escalas do escoamento turbulento em uma matriz de cilindros*. Master dissertation.

Tezuka, A.; Sunada, Y.; Rinoie, K. 2008. “Surface Pressure Distributions on 4% Circular Arc Airfoil at Low Reynolds Number”. *Journal of Aircraft*, Vol. 45, No. 6, p. 2164-2167.